

important to have sites from the two areas compared in the same laboratory.

21. Deformation features are directly correlated with peak shock pressure. Numerous studies show that moderate shock features (reduced refractive index, lamellar features) form at pressures between 20 and 40 GPa (depending on the rock type), and shock-fused quartz at pressures above 50 GPa. In turn, peak shock pressure is directly related to the particle velocity attained behind the shock. To a very good approximation in dry rocks, the velocity is doubled by the passing rarefaction [R. G. McQueen, S. P. Marsh, J. N. Fritz, *J. Geophys. Res.* **72**, 4999 (1967)]. For a peak shock pressure of 20 GPa, the measured shock velocities in 12 representative rocks are 0.8 to 1.4 km/s. The rarefaction velocities are then in the range of 1.6 to 2.8 km/s. Ahrens and Rosenberg [in *Shock Metamorphism of Natural Minerals*, B. French and N. Short, Eds. (Mono, Baltimore, MD, 1968), p. 59] extended the range of pressures to 45 GPa and measured all rarefaction (free surface) velocities to be less than 4.5 km/s. We therefore take 4.5 km/s as an upper limit on the velocity that could be attained by moderately shocked quartz grains launched by a simple cratering event in dry rocks. At higher pressures, higher rarefaction velocities are obtained, but the features of moderately shocked quartz are not preserved because the quartz is annealed or fused. Target rock texture (porosity in this case) and wetness also affect shock metamorphic features and rarefaction velocities [S. W. Kieffer, *J. Geophys. Res.* **76**, 5449 (1971)]. A significant effect for this discussion is that porosity and volatile content both increase the possible rarefaction velocities. For example, dry soil (~porous quartz soil) shocked to 30 GPa releases with a velocity of ~5.7 km/s, higher than that measured for single crystal or nonporous polycrystalline quartz. Wet soil shocked to the same pressure releases with a particle velocity of ~7.3 km/s [G. D. Anderson *et al.*, *Technical Report AFWL-TR-65-146* (SRI International, Menlo Park, CA, 1966)]. Thus, an impact into porous, water-saturated carbonates will produce products with significantly higher velocities than a similar impact into a dry, nonporous silicate target.
22. S. W. Kieffer and C. H. Simonds, *Rev. Geophys. Space Phys.* **18**, 143 (1980).
23. J. D. O'Keefe and T. J. Ahrens, *Geol. Soc. Am. Spec. Pap.* **190**, 103 (1982); *Nature* **338**, 247 (1989).
24. W. Alvarez, in (19). The necessary equations were modified from those given by A. Dobrovolskis [*Icarus* **47**, 203 (1981)]. His dimensionless parameters were converted to Earth's case as follows: 1 time unit = 806.3 s, 1 length unit = 6371 km, and 1 mass unit =  $5.973 \times 10^{27}$  g. Time-of-flight calculations follow those described by A. D. Dubyago [*The Determination of Orbits* (Macmillan, New York, 1961)].
25. The semimajor axis,  $a = 1/(2 - v^2)$  in dimensionless units, where  $v$  is the launch velocity.
26. P. H. Schultz and D. E. Gault, *Geol. Soc. Am. Spec. Pap.* **190**, 153 (1982).
27. V. R. Oberbeck, *Rev. Geophys. Space Phys.* **13**, 337 (1975).
28. H. J. Melosh, *Impact Cratering: A Geologic Process* (Univ. of Arizona Press, Tucson, 1988).
29. H. J. Melosh, N. M. Schneider, K. J. Zahnle, D. Latham, *Nature* **343**, 251 (1990).
30. D. J. Roddy *et al.*, *Int. J. Impact Eng.* **5**, 525 (1987); A. M. Vickery and H. J. Melosh, *Geol. Soc. Am. Spec. Pap.* **247**, 289 (1990).
31. The sensitivity of the impact cratering model to varying meteorite and target compositions and to impact velocity can be found in (22), especially tables 2 to 4, and figures 6 and 7. During the compression stage of an impact, peak shock pressure depends on the material properties of the meteorite and target and on the impact velocity. We ran a range of simulations for impact of a stony meteorite into targets of diabase, permafrost, carbonate, granite, and water [properties all given in (22)]. Peak pressures ranged from a minimum of 380 GPa (ice target) to 555 GPa (permafrost), to 657 GPa (granite), to 705 GPa (diabase). In all cases, energy was partitioned about half into the target and half into the meteorite during the compression stage. The ratio of penetration depth to

meteorite radius ranged from a minimum of 2.6 (diabase, carbonate, granite) to 3.2 (permafrost), to a maximum of 4.3 (liquid water).

32. K. O. Pope, K. H. Baines, A. C. Ocampo, B. A. Ivanov, *Earth Planet. Sci. Lett.* **128** (N3-4), 719 (1994).
33. E. López Ramos, *Geol. Mex.* **3**, 277 (1981). The "rocas volcánicas" mentioned on p. 277 are probably the impact melt rocks of the Chicxulub crater, not basement rock.
34. E. M. Jones and J. W. Kodis, *Geol. Soc. Am. Spec. Pap.* **190**, 175 (1982).
35. Continental positions calculated with the 66-Ma rotation parameters of the University of Chicago Paleogeographic Atlas Project, D. Rowley, personal communication.
36. At velocities greater than 10 km/s, ejecta can travel

farther west, but not farther east, so these are firm limits on the west edge of the forbidden zone for each elevation angle. Cusps in the boundaries of the forbidden zones are an artifact produced by joining segments of reimpact loci lines at 1-km/s increments.

37. P. H. Schultz, in (18), pp. 105-106.
38. We thank J. Bostwick and F. T. Kyte for discussion and for a preprint of their work on the K-T boundary of the Pacific plate and D. Rowley for plate-rotation parameters. Comments by R. Jeanloz and C. Koeberl on an earlier version of this manuscript are greatly appreciated. Supported by the National Aeronautics and Space Administration (NASA) grant NAGW-3008 and NSF grant EAR-91-05297 to W.A., NASA grant NAGW-1740 to S.W.K., and University of California Berkeley Esper A. Larsen Jr. Research Fund.

# Resonance Light Scattering: A New Technique for Studying Chromophore Aggregation

Robert F. Pasternack and Peter J. Collings

Light scattering experiments are usually performed at wavelengths away from absorption bands, but for species that aggregate, enhancements in light scattering of several orders of magnitude can be observed at wavelengths characteristic of these species. Resonance light scattering is shown to be a sensitive and selective method for studying electronically coupled chromophore arrays. The approach is illustrated with several examples drawn from porphyrin and chlorin chemistry. The physical principles underlying resonance light scattering are discussed, and the advantages and limitations of the technique are reviewed.

We have recently reported (1) on a new resonance technique called resonance light scattering (RLS) that is both extremely sensitive and selective in probing chromophore aggregation in a number of different systems. The theory behind this technique is not new, and in fact RLS has been tried in the past for purposes other than studying aggregation. In those cases, the technique was only marginally successful. However, we have found that in aggregation experiments, RLS not only meets sensitivity and selectivity criteria but offers the additional benefits of simplicity and versatility. In this article, we describe the basic physics behind RLS, survey some ongoing research on its refinement and application to different systems, and discuss a number of areas in which RLS may make important contributions in the near future.

## Experimental Approaches to Studying Aggregation

The recent flurry of research activity on supramolecular assemblies and their application in the construction of nanodevices has

encouraged the development of experimental techniques capable of detecting and characterizing these assemblies. Understanding the chemical, biological, and pharmacological activity of a complex system requires knowledge of the state of molecular aggregation of the system's components. Research issues that involve relations between the properties of complex systems and the formation of large aggregates include (i) the organization of chlorophyll and other pigments in chlorosomes, in which a particular molecular assembly is required for efficient photosynthesis (2); (ii) the relation of photosensitization efficiency to the extent of aggregation of the active component at cancer cells, which must be resolved to enable rational design of alternative reagents in photodynamic cancer therapy (3); and (iii) the state of aggregation of lipids and drugs in liposomes, which has been shown in certain cases to be a crucial factor in their effectiveness in treating disease (4). Although light scattering experiments are frequently used to study such problems, in these three examples conventional light scattering would likely not yield useful data because of the background signals provided by the medium; not only the existence but the identity of the scatterer must be determined.

Even though light scattering experiments

R. F. Pasternack is in the Department of Chemistry and P. J. Collings is in the Department of Physics and Astronomy at Swarthmore College, 500 College Avenue, Swarthmore, PA 19081, USA.

typically involve measurements away from absorption bands, wavelengths within the absorption band envelope can be extremely informative if the absorption is not too great and the aggregate is of sufficient size. The RLS effect is observed as increased scattering intensity at or very near the wavelength of absorption of an aggregated molecular species. The effect can be enhanced by several orders of magnitude when strong electronic coupling exists among the chromophores. In addition, the wavelength dependence of this technique allows for selective observation of aggregates, even in multicomponent systems that include a large fraction of monomers or other aggregates. Moreover, in many cases RLS experiments can be conducted with conventional equipment; our initial experiments were done with an ordinary double-monochromator fluorimeter under software control.

### An Application of RLS to Arrays

In 1993, we first applied RLS to the study of chromophore arrays (1). In studies of the interactions of cationic porphyrins (including their metal derivatives) with nucleic acids, we found that these species can bind to DNA by intercalation, external groove binding, or both, and that the type of binding depended on porphyrin structure and polynucleotide composition (5). Of the various spectroscopic and kinetic methods for investigating relations among structure, binding mode, and base pair preference, none proved to be more useful than circular dichroism (CD). Induced CD signals for the binding of one such cationic porphyrin derivative with DNA could best be accounted for in terms of an extended, electronically coupled array of porphyrin molecules on the surface of the DNA (6). Although it was apparent from these measurements that the porphyrin was assembled in some extended manner that involved periodic repeats, the state of aggregation of the DNA was less certain. A variety of indirect evidence supported the dispersed nature of the DNA, but it was not until RLS was applied that this issue could be resolved.

To illustrate the method, we compared results obtained for neat water and two porphyrins that do not form extended aggregates in aqueous solution (Fig. 1A) to the results for an aggregating porphyrin termed  $t\text{-H}_2\text{P}_{\text{agg}}$  (Fig. 1B). Figure 1A shows no enhanced scattering at the absorption bands of the porphyrins; rather, minima appear as a result of absorption in the Soret region of the photons of the incident and scattered radiation. In contrast, Fig. 1B shows results typical for a porphyrin array; the intensity of the scattered light is orders of magnitude greater than that obtained for water or nonaggregating porphyrins. The

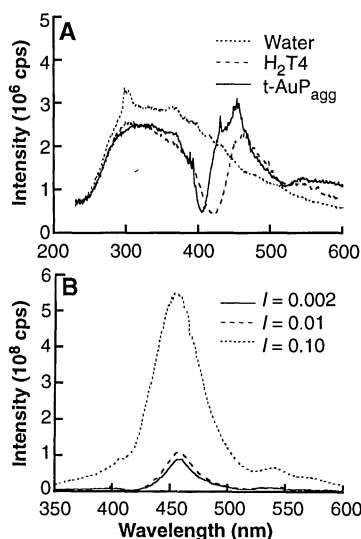


**Fig. 1.** (A) RLS profiles of water and two nonaggregating porphyrin derivatives, 5  $\mu\text{M}$   $\text{H}_2\text{T4}$  and 5  $\mu\text{M}$   $t\text{-AuP}_{\text{agg}}$ . (B) RLS profiles of 5  $\mu\text{M}$   $t\text{-H}_2\text{P}_{\text{agg}}$ , an aggregating porphyrin, as a function of ionic strength  $I$ . Spectra are not corrected for photomultiplier response. [Reprinted from (1) with permission of the American Chemical Society]

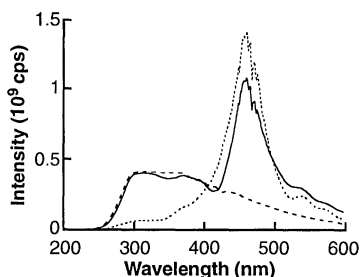


**Fig. 2.** Light scattering measurements of DNA and  $t\text{-H}_2\text{P}_{\text{agg}}$ -DNA complexes. Dashed line, DNA condensed with hexaamminecobalt(III); solid line,  $t\text{-H}_2\text{P}_{\text{agg}}$  added to DNA previously condensed with hexaamminecobalt(III); dotted line,  $t\text{-H}_2\text{P}_{\text{agg}}$ -DNA complex to which no hexaamminecobalt(III) was added. Spectra are not corrected for photomultiplier response. [Reprinted from (1) with permission of the American Chemical Society]

peak is centered near the absorption band maximum of the aggregate.

The light scattering results for  $t\text{-H}_2\text{P}_{\text{agg}}$  in its complexes with DNA are shown in Fig. 2. DNA that was condensed by the addition of hexaamminecobalt(III) under low-salt conditions scattered light extensively in the ultraviolet (UV) region (dashed line in Fig. 2). When  $t\text{-H}_2\text{P}_{\text{agg}}$  was added to this aggregated DNA, an enhanced RLS profile was obtained in the Soret region between 400 and 500 nm (solid line in Fig. 2). The UV scattering profile attributable primarily to DNA, which was still in a condensed state, was almost unaffected. Comparison of these two profiles to one obtained in the UV region for a  $t\text{-H}_2\text{P}_{\text{agg}}$ -DNA solution in which the DNA

was not previously condensed with hexaamminecobalt(III) (dotted line in Fig. 2) shows that the porphyrin alone is not capable of aggregating the nucleic acid. Thus, the combination of CD and RLS measurements provides a very powerful experimental strategy for the study of chromophore assemblies and, in this case, confirms the model put forth for DNA-bound porphyrin arrays. The CD method yields porphyrin signals characteristic of long-range periodic repeats when the (symmetrical) chromophore is bound to the polymer, whereas the RLS method is extremely sensitive to aggregate formation and discriminates between polymer-backbone aggregates and bound chromophore aggregates.

### Theory of RLS

In general, two processes occur when light passes through a solution of aggregates. If the solvent itself is nonabsorbing, then energy is removed from the incident light through absorption and scattering by the aggregates. The light scattering component is a consequence of differences in polarizability between the aggregates and the solvent. The incident electromagnetic wave induces an oscillating dipole in the assembly, which radiates light in all directions. The ratio of the rate of energy absorption from the incident beam to the intensity of the incident beam is called the absorption cross section,  $C_{\text{abs}}$ . The ratio of the rate of energy scattering out of the incident beam (in all directions) to the intensity of the incident beam is called the scattering cross section,  $C_{\text{sca}}$ . If the induced dipole can be considered ideal—which is usually a valid assumption if the size of the aggregate is small compared to the wavelength of the light in the solvent,  $\lambda_m$ —both cross sections are related to the polarizability of the aggregates in simple ways,

$$C_{\text{abs}} = k_m \alpha_i \quad (1)$$

$$C_{\text{sca}} = \frac{k_m^4}{6\pi} |\alpha|^2 = \frac{k_m^4}{6\pi} (\alpha_r^2 + \alpha_i^2) \quad (2)$$

where  $k_m$  is the wave vector of light in the solvent,  $k_m = 2\pi/\lambda_m$ , and  $\alpha_r$  and  $\alpha_i$  are the real and imaginary parts of the polarizability of the aggregates. Absorption at a certain wavelength band by a solution of aggregates can be understood as the result of a maximum in the imaginary part of the polarizability in that region of the spectrum; the absorbance  $A$  of a sample of thickness  $L$  is

$$A = 2.3^{-1} \left( \frac{N}{V} \right) C_{\text{abs}} L \quad (3)$$

where  $N/V$  is the number of aggregates per unit volume. The real and imaginary parts of  $\alpha$  are related to each other, so that when

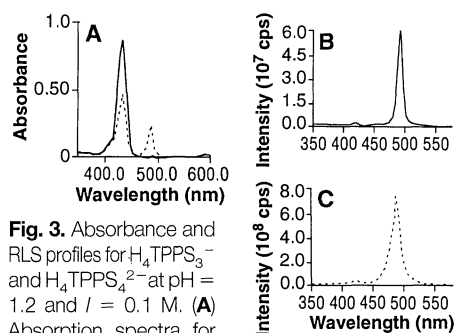


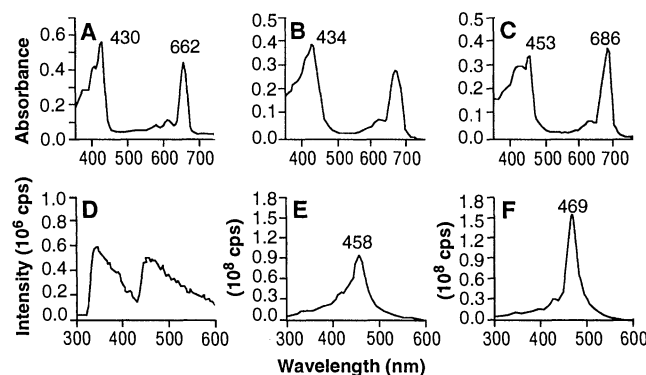
**Fig. 3.** Absorbance and RLS profiles for  $H_4TPPS_3^-$  and  $H_4TPPS_4^{2-}$  at pH = 1.2 and  $I = 0.1$  M. (A) Absorption spectra for  $H_4TPPS_3^-$  (dashed line) and  $H_4TPPS_4^{2-}$  (solid line). (B) RLS profile for  $H_4TPPS_4^{2-}$ . (C) RLS profile for  $H_4TPPS_3^-$ . Spectra are not corrected for photomultiplier response. [Reprinted from (19) with permission of the American Chemical Society]

$\alpha_i$  is maximized in some wavelength range,  $\alpha_r$  also behaves anomalously in this region; hence,  $|\alpha|^2$  is at a maximum in the absorption band, which also results in increased scattering.

Under normal conditions this increased scattering is difficult or impossible to detect because of the increased absorption and the weakness of the enhanced scattering effect. However, when this effect is investigated for aggregates of chromophores, the enhanced RLS scattering can be enormous. The absorption depends on the first power of the polarizability, which in turn depends linearly on the volume of the aggregate. Thus, a solution with a fixed concentration of the aggregating component will exhibit no change in  $A$  as aggregation occurs, because the product of  $N/V$  and  $\alpha_i$  remains constant. However, the amount of scattering depends on the square of the volume of the aggregate, and thus it increases as a consequence of aggregation; RLS is therefore extremely sensitive to even low concentrations of extended aggregates.

The ideas behind RLS are not new; they are discussed in a number of classical texts on light scattering, which often include a comment concerning the effect of absorption on the scattering cross section. During the past 20 years, theoretical and experimental researchers have attempted to predict the enhancement precisely and to observe it in a number of systems. The theoretical work focused on fluctuation theory (7) and semiclassical calculations (8); the experiments were performed on diphenylpolyenes (9), lycopine (10),  $\beta$ -carotene (11), coumarin dyes and 3,4-dinitrophenol (8), dibenzoylmethane complexes (12), and cyanine dyes (13). Dynamic light scattering measurements were performed on nitrophenolate anions (14), iodine (15), and heme proteins (16). These experiments included measurements just outside the absorption band (preresonance scattering) and within the absorption band. The experiments allowed

**Fig. 4.** Absorption and RLS spectra of chlorophyll *a* in solution. (A through C) Absorption spectra of 5  $\mu$ M chlorophyll *a* in (A) acetone; (B) formamide:buffer, 4 min after mixing; and (C) formamide:buffer, 60 min after mixing. (D through F) RLS spectra of 5  $\mu$ M chlorophyll *a* in (D) acetone; (E) formamide:buffer, 7 min after mixing; and (F) formamide:buffer, 123 min after mixing. Spectra are not corrected for photomultiplier response. [Reprinted from (20) with permission of the Biophysical Society]



the measurement of reorientation times and hydrodynamic radii on the basis of the enhanced light scattering observed, and they verified that the complexes were predominantly in monomeric form. The amount of light scattering was not very large in any of these experiments because the absorbing species did not form aggregates with good electronic coupling among the chromophores under any of the experimental conditions. Such coupling seems to be crucial for substantial signal enhancement to occur.

### Other Examples of RLS

The extreme sensitivity of RLS as a tool for measuring chromophore aggregation is illustrated by a study of the diacid forms of the water-soluble anionic porphyrins, tetraphenylporphinesulfonates ( $H_4TPPS_4^{2-}$  and  $H_4TPPS_3^-$ ). The absorption spectrum of these porphyrins in the Soret region at pH 1 is shown in Fig. 3. We previously described the appearance of an "anomalous" band at 489 nm for  $H_4TPPS_3^-$  and suggested a connection to porphyrin aggregation (17). Later studies identified this band as arising from a J-aggregate of porphyrin moieties, that is, an extended assembly involving monomer units partially offset from near neighbors (18). Under the conditions of the experiment shown in Fig. 3, the ratio of the intensities of the Soret bands (arising from monomer at 434 nm and aggregate at 489 nm) is about 100:1 for  $H_4TPPS_4^{2-}$ . However, the light scattering profile is dominated by the relatively small amount of aggregate present. The RLS technique successfully reports and identifies aggregated species even at very low concentrations (19).

The selectivity of RLS proved invaluable for mechanistic studies of chlorophyll *a* aggregation (20). Figure 4 shows the absorbance and RLS profiles of chlorophyll *a* in acetone, where it is monomeric, and in 9:1 formamide:phosphate buffer, which fosters its aggregation. As the chlorophyll aggregates, high scattering intensity is observed, first at 458 nm and subsequently at 469 nm.

The  $Chl_{458}$  species has only weak CD features, whereas the equilibrium CD profile is characteristic of an extended organized array. The data suggest a mechanism for aggregation that begins with the formation of small oligomers that provide neither CD nor RLS signals beyond background (incubation period), followed by the formation of an intermediate, which is a very large aggregate that has an electronic transition between 458 and 461 nm ( $Chl_{458}$ ) but is not extensively chiral. The CD and RLS spectra obtained 2 hours after mixing both show strong features centered at  $\sim 469$  nm. We proposed that this species,  $Chl_{469}$ , is formed by the folding of the large aggregate initially produced in this medium ( $Chl_{458}$ ) into a chiral structure. This application of the RLS method enabled us to identify the intermediate as a large aggregate different from the final product and to discern its mechanistic implications for an aggregate conformational change.

Although the examples given thus far have involved porphyrins and the closely related chlorins, enhanced RLS signals are not restricted to macrocyclic chromophores. We have obtained large RLS features for acridine and cyanine dyes and even for a square planar platinum complex (21) under conditions in which they are extensively aggregated. In these cases, enhanced signals appear to require an extended array of electronically coupled chromophores having a large oscillator strength, rather than chromophores with a particular structural feature. Nor is it necessary for the chromophores in the assembly to be identical; enhanced RLS signals have recently been obtained for a heteroaggregate system (22).

### Dynamic Light Scattering

Particle size measurement techniques that have been developed for conventional light scattering can also be applied to RLS. Dynamic light scattering (DLS) measures the frequency spectrum of the scattered light. The relaxation time for fluctuations in the scattered light (the inverse of the line

width) depends only on the diffusion behavior of the aggregates. For spherical aggregates, the translational diffusion constant  $D$  is given by the Stokes-Einstein relation

$$D = \frac{kT}{6\pi\eta r} \quad (4)$$

where  $k$  is Boltzmann's constant,  $T$  is the absolute temperature,  $\eta$  is the viscosity of the solution, and  $r$  is the hydrodynamic radius of the aggregate. The relaxation time  $\tau$  is simply

$$\tau = (2Dq^2)^{-1} \quad (5)$$

where  $q = 2k_m \sin(\theta/2)$  and  $\theta$  is the scattering angle (23). Measurement of  $\tau$  therefore determines the hydrodynamic radius of the aggregates, provided the temperature and viscosity of the solvent are known.

Depolarized DLS experiments allow determination of both the size and shape of the aggregates. The above relations are valid for nonspherical aggregates if vertically polarized light is incident and only vertically polarized scattered light is detected. The relaxation time in this condition,  $\tau_{VV}$ , can be used to find  $D$  by means of

$$\tau_{VV} = (2Dq^2)^{-1} \quad (6)$$

If vertically polarized light is incident and horizontally polarized scattered light is detected, then the relaxation time  $\tau_{VH}$  depends on both  $D$  and the rotational diffusion constant  $\Theta$  according to

$$\tau_{VH} = (2Dq^2 + 12\Theta)^{-1} \quad (7)$$

(24). Measurements of  $\tau_{VV}$  and  $\tau_{VH}$  therefore determine  $D$  and  $\Theta$ , which in turn depend on the size and shape of the aggregate. For example, the model of Riseman and Kirkwood calculates  $D$  and  $\Theta$  for rods of length  $L$  and diameter  $d$ ,

$$D = \frac{kT}{3\pi\eta L} \ln\left(\frac{L}{d}\right) \quad (8)$$

$$\Theta = \frac{3kT}{\pi\eta L^3} \ln\left(\frac{L}{d}\right) \quad (9)$$

(25). Thus there is a one-to-one relation between  $(L, d)$  and  $(\tau_{VV}, \tau_{VH})$ , so that measurements of the latter allow the former to be calculated.

We applied these ideas to the measurement of aggregate size with the diacid form of tetraphenylporphinesulfonate ( $H_4TPPS_3^-$ ) whose (aggregate) absorption peak is near 488 nm, the wavelength of the 10-mW laser in our DLS system (see Fig. 3). A 3  $\mu$ M solution of this porphyrin aggregates when the concentration of HCl reaches 0.02 M. This is illustrated in Fig. 5 by the increase in the intensity of scattered light. The relaxation time  $\tau_{VV}$  for the vertical-vertical polarization arrangement is also shown. These times were measured with the correlator set

for a 15- $\mu$ s sampling time; excellent correlation functions were obtained after  $\sim 10$  min. Note that the relaxation time does not change during the aggregation process. Because  $\tau_{VV}$  depends only on the translational diffusion constant  $D$ , which in turn is determined by both the length and diameter of the aggregates, a constant value of  $\tau_{VV}$  implies that the dimensions of the aggregates do not change markedly as more aggregates form.

Our preliminary measurements of the depolarization ratio  $\rho_V(90)$  (the ratio of horizontally polarized light to vertically polarized light scattered at  $90^\circ$ , with the incident light being vertically polarized) also support the conclusion that the aggregate size does not change during the aggregation process, that is,  $\rho_V(90)$  remains  $\sim 0.25$  as HCl is added. An isotropic scatterer with three equal principal components of the polarizability tensor gives  $\rho_V(90) = 0$ , whereas a scatterer with one principal component much greater than the other two gives  $\rho_V(90) = 0.33$  in the ideal dipole approximation (26). Therefore, these results indicate that the  $H_4TPPS_3^-$  aggregates are characterized by one fairly large polarizability component, which is not surprising in light of the stacking arrangements that are typical of aggregating porphyrins (18).

We have performed a few depolarized DLS experiments on  $H_4TPPS_3^-$ , and the results are very encouraging. In an experiment in which HCl was titrated into the solution with depolarized DLS measurements after each addition, the length and diameter of the aggregates remained  $\sim 600$  nm and  $\sim 15$  nm, respectively, despite a large increase in the intensity of the scattered light. In a subsequent experiment in which a 0.03 M HCl solution was used, the

aggregates remained  $\sim 900$  nm long and  $\sim 10$  nm in diameter over a period of nearly 3 hours. Although these results are preliminary, they illustrate the power of RLS as a tool for determining the size and shape of aggregates. Much additional work needs to be done, especially at angles other than  $90^\circ$ , to show the dependence of these relaxation times on the scattering vector.

## Experimental Limitations

The signal-to-noise ratio for RLS falls off markedly in experiments that are conducted in the presence of very large aggregates that produce large conventional Rayleigh signals. For example, dyed latex microspheres produce an RLS signal that is barely detectable above background, and a similar result is obtained for porphyrin aggregates in a liposome-containing medium. The situation is similar to that encountered in studies of latex spheres with silver "islands" on them (27). Moreover, the systems we have thus far discussed are either nonfluorescent or fluoresce at wavelengths far removed from the wavelength of RLS detection. Many chromophore assemblies of interest do not meet either condition, and a technique needs to be developed to distinguish among photons that are scattered and those that arise from luminescence. Finally, our experiments have been done almost exclusively with right-angle detection, with a fluorimeter or a laser system that has a fixed-angle geometry. Studies of highly absorbing systems will require an ability to change the angle of detection, preferably without markedly increasing the background scattering. In collaboration with colleagues at the University of Messina, we have attempted one experiment at non- $90^\circ$  detection, and the results encourage us to believe that the experimental design can be optimized to suit the requirements of individual samples.

## Future Applications

Although RLS is clearly in its infancy, this technique has many potential applications. The experimental approach can be expanded to include time-resolved measurements or backscattering geometries. Time-resolved RLS methods will be particularly helpful for the study of the dynamics of energy and electron transfer in chromophore arrays, for which absorption techniques are not very sensitive and for which fluorescence yields are generally very low. Measurements in near-backscattering geometries open the possibility of working with nearly opaque samples or thin films. Such an experimental approach would be useful for probing the state of aggregation of

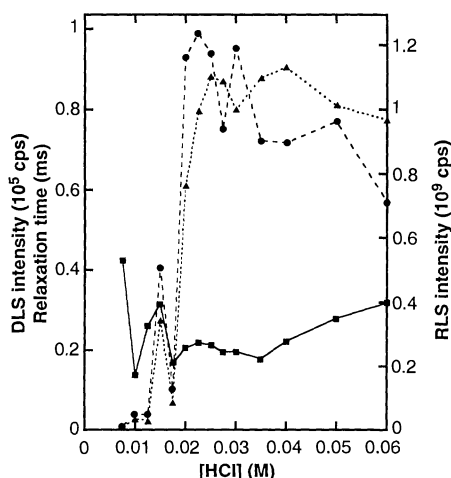


Fig. 5. DLS intensity (●) and relaxation time (■) for  $H_4TPPS_3^-$  as a function of HCl concentration. The RLS intensity profile measured by the fluorimeter (▲) is also shown.

chromophores in organelles of cells or of aggregates in sensor arrays.

Colloidal and aerosol systems are amenable to the use of RLS. For example, small metal particles have peaks in  $C_{\text{abs}}$  and  $C_{\text{sca}}$  at specific wavelengths; these peaks are not the result of absorption by the material but arise from naturally occurring electromagnetic resonances associated with surface plasmon modes. Information on particle size and shape can be obtained even in colloidal and aerosol systems containing particles of very different sizes or particles composed of different materials. Nor is the use of RLS restricted to the visible part of the spectrum; in particular, because many compounds have narrow infrared absorption bands, enhanced light scattering may also occur at these wavelengths. These possibilities are representative of the types of systems in which RLS may make an important contribution. The enhancement of Rayleigh scattering resulting from absorption is a very general phenomenon and therefore

may provide important experimental opportunities in a wide range of areas.

## REFERENCES

1. R. F. Pasternack, C. Bustamante, P. J. Collings, A. Giannetto, E. J. Gibbs, *J. Am. Chem. Soc.* **115**, 5393 (1993).
2. R. E. Blankenship, D. C. Brune, B. P. Wittmerhaus, in *Light-Energy Transduction in Photosynthesis: Higher Plant and Bacterial Models*, S. E. Stevens Jr. and D. A. Bryant, Eds. (American Society of Plant Physiologists, Rockville, MD, 1988), pp. 32–46.
3. T. J. Dougherty, in *Advances in Photochemistry*, D. H. Volmar, G. S. Hammond, D. C. Neckers, Eds. (Wiley, New York, 1992), pp. 275–311.
4. W. R. Perkins *et al.*, *Biochim. Biophys. Acta* **1107**, 271 (1992).
5. R. F. Pasternack, E. J. Gibbs, J. J. Villafranca, *Biochemistry* **22**, 2406 (1983).
6. E. J. Gibbs, I. Tinoco Jr., M. F. Maestre, P. A. Ellinas, R. F. Pasternack, *Biochem. Biophys. Res. Commun.* **157**, 350 (1988).
7. G. A. Miller, *J. Phys. Chem.* **82**, 616 (1978).
8. S. G. Stanton, R. Pecora, B. S. Hudson, *J. Chem. Phys.* **75**, 5615 (1981).
9. D. R. Bauer, B. S. Hudson, R. Pecora, *ibid.* **63**, 588 (1975).
10. J. Anglister and I. Z. Steinberg, *Chem. Phys. Lett.* **65**, 50 (1979).
11. ———, *J. Chem. Phys.* **74**, 786 (1981).
12. W. H. Nelson, W. F. Howard, R. Pecora, *Inorg. Chem.* **21**, 1483 (1982).
13. J. Anglister and I. Z. Steinberg, *J. Chem. Phys.* **78**, 5358 (1983).
14. S. G. Stanton, R. Pecora, B. S. Hudson, *ibid.*, p. 3365.
15. J. V. Magill and J. H. R. Clarke, *J. Phys. Chem.* **89**, 734 (1985).
16. R. Chiarello and L. Reinisch, *J. Chem. Phys.* **88**, 1253 (1988).
17. R. F. Pasternack *et al.*, *J. Am. Chem. Soc.* **94**, 4511 (1972).
18. D. L. Akins, H.-R. Zhu, C. Guo, *J. Phys. Chem.* **98**, 3612 (1994).
19. R. F. Pasternack, K. F. Schaefer, P. Hambright, *Inorg. Chem.* **33**, 2062 (1994).
20. J. C. de Paula, J. H. Robblee, R. F. Pasternack, *Biophys. J.* **68**, 335 (1995).
21. G. Arena, L. Monsu Scolaro, R. F. Pasternack, R. Romeo, *Inorg. Chem.* **34**, 2994 (1995).
22. R. F. Pasternack, R. Purrello, E. Gibbs, O. Vafeek, P. J. Collings, unpublished data.
23. N. C. Ford, in *Dynamic Light Scattering*, R. Pecora, Ed. (Plenum, New York, 1985), pp. 7–58.
24. K. Zero and R. Pecora, *ibid.*, pp. 59–83.
25. J. Riseman and J. G. Kirkwood, *J. Chem. Phys.* **18**, 512 (1950).
26. C. F. Bohren and D. R. Huffman, *Absorption and Scattering of Light by Small Particles* (Wiley, New York, 1983).
27. P. A. Schuele *et al.*, *Anal. Chem.* **65**, 3177 (1993).

# AAAS–Newcomb Cleveland Prize

## To Be Awarded for a Report, Research Article, or an Article Published in *Science*

The AAAS–Newcomb Cleveland Prize is awarded to the author of an outstanding paper published in *Science*. The value of the prize is \$5000; the winner also receives a bronze medal. The current competition period began with the 2 June 1995 issue and ends with the issue of 31 May 1996.

Reports, Research Articles, and Articles that include original research data, theories, or syntheses and are fundamental contributions to basic knowledge or technical achievements of far-reaching consequence are eligible for consideration for the prize. The paper must be a first-time publication of the author's own work. Reference to pertinent earlier work by the author may be included to give perspective.

Throughout the competition period, readers are

invited to nominate papers appearing in the Reports, Research Articles, or Articles sections. Nominations must be typed, and the following information provided: the title of the paper, issue in which it was published, author's name, and a brief statement of justification for nomination. Nominations should be submitted to the AAAS–Newcomb Cleveland Prize, AAAS, Room 924, 1333 H Street, NW, Washington, DC 20005, and **must be received on or before 30 June 1996**. Final selection will rest with a panel of distinguished scientists appointed by the editor-in-chief of *Science*.

The award will be presented at the 1997 AAAS annual meeting. In cases of multiple authorship, the prize will be divided equally between or among the authors.